Biochemical and Biophysical Research Communications xxx (xxxx) xxx

Contents lists available at ScienceDirect

Biochemical and Biophysical Research Communications

journal homepage: www.elsevier.com/locate/ybbrc

Salt concentration modulates the DNA target search strategy of NdeI

Raquel M. Ferreira [a], Anna D. Ware [a], Emily Matozel [a], Allen C. Price [b, *]

[a] Department of Biology, Emmanuel College, 400 the Fenway, Boston, MA, 02115, United States
[b] Department of Chemistry and Physics, Emmanuel College, 400 the Fenway, Boston, MA, 02115, United States

ARTICLE INFO

Article history:
Received 2 October 2020
Accepted 14 October 2020
Available online xxx

Keywords:
Restriction endonucleases
DNA
Single molecule
Facilitated diffusion
DNA target Search

ABSTRACT

DNA target search is a key step in cellular transactions that access genomic information. How DNA binding proteins combine 3D diffusion, sliding and hopping into an overall search strategy remains poorly understood. Here we report the use of a single molecule DNA tethering method to characterize the target search kinetics of the type II restriction endonuclease NdeI. The measured search rate depends strongly on DNA length as well as salt concentration. Using roadblocks, we show that there are significant changes in the DNA sliding length over the salt concentrations in our study. To explain our results, we propose a model including cycles of 3D and 1D search in which salt concentration modulates the strategy by varying the length of DNA probed per 1D scan. At low salt NdeI makes a single non-specific encounter with DNA followed by an effective and complete 1D scan. At higher salt, NdeI must execute multiple cycles of target search due to the reduced efficacy of 1D search.

1. Introduction

Site specific DNA binding proteins (DBPs) slide, hop and jump along DNA during target search [1–3]. A DBP must combine these mechanisms of facilitated diffusion into a coherent strategy in order to systematically reject the wrong DNA while maintaining the ability to recognize target DNA. Strategies vary widely. LacI uses long sliding interactions in its search for its binding site [4–6]. EcoRI mixes sliding and hopping as well as pausing at star sites [7–9]. In contrast, RNA polymerase [10] as well as the UV damaged DNA binding protein [11] have been shown to find their sites via 3D diffusion alone.

Type II restriction endonucleases (REs) are a useful model for studying target search [12,13]. Facilitated diffusion in REs was first observed in EcoRI [14] and later in BamHI, HindIII [15] and EcoRV [16]. These early studies used bulk assays with cleavage products analyzed by gel electrophoresis. Search rates at low salt concentration increased with DNA length suggesting sliding [15]. Target search by EcoRV is enhanced by the presence of nearby topologically disconnected DNA catenenes, indicating jumping plays a role [17]. The dependence of coordinated cleavage of multiple sites on spacing and orientation demonstrates that 1D diffusion is a combination of both sliding and hopping [9,16,18].

How the target search rate depends on DNA length and conformation as well as cellular or buffer conditions is determined by the search strategy. For example, the LacI search rate with shorter DNAs (<7 kbp) is independent of salt concentration at low salt, but rapidly decreases as salt is increased past a critical concentration. On the other hand, longer DNAs show a peak in rate as salt is varied, a behavior explained by a model that includes sliding [4]. A study of LacI association kinetics *in vivo* showed that placement of roadblocks on one side of the target reduced the overall search rate to roughly one half, confirming sliding *in vivo* [5]. By stretching a DNA substrate between two optically trapped beads and measuring the search rate *in singulo*, Van der Broek et al. have shown that target search by EcoRV depends on bead separation, and hence DNA conformation, further confirming the presence of jumping during search [19].

In this work, we use a single molecule technique based on DNA tethered beads to measure the target search rate of NdeI, a type II RE, under a wide range of salt concentrations and for two DNA substrate lengths. The advantage of single molecule techniques is that they measure the underlying distributions of molecular properties, as opposed to ensemble averages [20]. In addition, DNA tethering methods can modify the tension and conformation of DNA [19,21]. We have previously measured an effective second order rate constant of $(3.3 \pm 0.4) \times 10^8\ M^{-1}\ s^{-1}$ for target search by this enzyme, a value consistent with a diffusion controlled reaction [22]. Here we demonstrate that this rate is highly dependent on salt concentration and DNA length. For each DNA length, we see a peak in search rate as salt is increased from 2 mM to 160 mM. The peak in rate is DNA length dependent, with the peak rate increasing and

* Corresponding author.
E-mail address: priceal@emmanuel.edu (A.C. Price).

https://doi.org/10.1016/j.bbrc.2020.10.036
0006-291X/

Abbreviations

RE	restriction endonuclease
bp	base pair
DBP	DNA binding protein
PCR	polymerase chain reaction

shifting to lower salt concentration for longer DNAs. In addition, we use dCas9 as a roadblock to demonstrate that increased salt concentration can reduce the sliding length. To explain our data, we propose a model of 3D/1D search cycles that is modulated as the 1D search efficacy varies with salt concentration. The model shows that at low salt NdeI makes a single encounter with the DNA followed by a highly effective scan of the entire DNA. At high salt, NdeI must make multiple short scans of the DNA during target search.

2. Materials and methods

2.1. DNA substrate preparation

Linear DNAs were prepared using a polymerase chain reaction (PCR) with custom primers (Integrated DNA Technologies (IDT)) labeled on the 5′ end with either biotin or digoxigenin. M13mp18 circular plasmid (New England Biolabs (NEB)) was used as template DNA. The 1000 bp linear DNA was prepared as described previously [22] and consists of the circular M13mp18 sequence from position 6338 to 107. For the 200 bp DNA, the forward primer (digoxigenin labeled) was AGCTGATTTAACAAAAATTTAATGCGA, and the reverse primer (biotin labeled) was TGAGAGATCTACAAAGGCTATCAG, copying the template DNA from position 6725 to 7012. Both PCR products contain a single NdeI cleavage site at the center of the DNA (Fig. 1A). PCR products were purified as described in Ref. [22]. DNAs were diluted to 0.5–1.5 pM in buffer A (20 mM Tris-HCl pH 7.5, 2–60 mM NaCl, 3 mg/mL BSA, 1 mg/mL Pluronic F-127, 0.2–2.0 mM $MgCl_2$) for use in tethering.

2.2. Sample cell preparation

Sample flow cells were constructed and functionalized with anti-digoxigenin FAB fragments as described in Refs. [22]. The microfluidic cell was mounted on an inverted microscope (Axiovert, Zeiss) and connected to a syringe pump (Harvard Instruments).

2.3. DNA tethering

DNA tethering for the target search rate experiments was achieved using the method described in Refs. [22]. Briefly, this method involved flowing in DNA first, and then flowing in 1 μm diameter streptavidin functionalized beads (MyOne Streptavidin, Life Technologies) to bind to the tethered DNA (Fig. 1B). Wash steps followed both the DNA and the bead binding steps. For control and roadblock experiments, binding of DNA to beads was achieved by the method described in Ref. [23]. In this method, beads were reacted with DNA before injection into the flow channel followed by a single wash step. Both tethering protocols yield similar tethering and experiments repeated using both protocols gave equivalent results.

2.4. Data collection

For the search rate and roadblock measurements, the site-specific endonuclease NdeI (NEB) was diluted to 1 U/mL (42 pM) in buffer A and flowed into the reaction channel of the flow cell at 10 μL/min. Video data was collected under dark field illumination for 30–90 min (depending on cleavage rate) at a frame rate of 1 fps. For the control experiments, inlet channels were switched to wash buffer (buffer A with 80 mM NaCl and 2 mM $MgCl_2$) at 6 min into data collection.

2.5. Data analysis

Data reduction was performed as previously described [22,23]. Briefly, beads in each frame were counted using the ImageJ Particle Analysis plugin (Fig. 1C). Baseline subtracted and normalized bead count versus time curves were plotted and fit to single exponentials, $P(t) = Ae^{-kt}$, where $P(t)$ is the fraction of uncleaved DNAs at time t, A is the amplitude, and k is the first order rate of site-specific DNA cleavage. The effective second order rate constants were calculated by dividing the measure first order cleavage rates by the protein concentration (42 pM). Fitting of the kinetic model for target search was done as follows. The measured first order search rates were plotted versus salt concentration for both lengths of DNA. Equation (1) was fit globally to our data using non-linear least squares fitting (Marquardt-Levenberg algorithm). The reference salt concentration was chosen as $[NaCl]_o = 100$ mM. The parameters q and a were globally fit to all data (both lengths of DNA). The parameters τ^o_{3D} and N_o were assumed to be length dependent and allowed to vary between the data corresponding to the two DNA lengths.

3. Results

3.1. Measurements of DNA target search rate

To characterize the target search kinetics of NdeI, we used our single molecule DNA cleavage assay (Fig. 1). We previously showed that NdeI's second order rate constant is $(3.3 \pm 0.4) \times 10^8$ M^{-1} s^{-1} for 1000 bp DNAs in 100 mM NaCl, a value within the range of diffusion controlled reactions [22]. In order to change the target search kinetics, in this work we varied both salt concentration

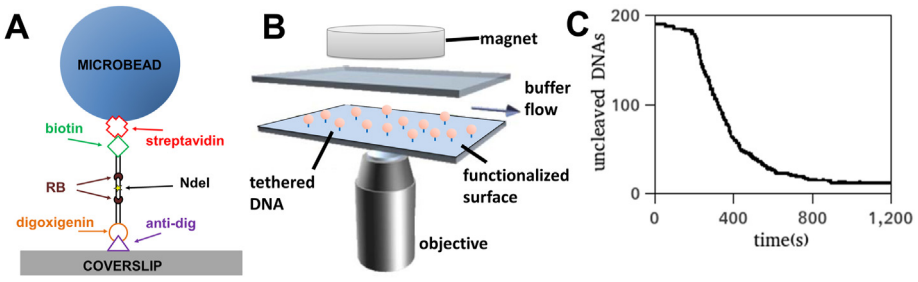

Fig. 1. Single molecule DNA cleavage assay. (A) DNA tethering details. NdeI and roadblock (RB) sites are labeled. (B) Tethered microbeads are cleaved by enzymes introduced by flow. (C) Number of uncleaved DNAs versus time. Initial slow decay is due to background bead loss. The decay rate after ~200 s is due to enzyme catalyzed cleavage.

(2 mM–160 mM) and DNA length (200 bp to 1000 bp). Increasing salt concentration increases non-specific DNA dissociation and hence reduces time spent during 1D scanning and changing DNA length will increase the amount of DNA that must be scanned during search.

Fig. 2 shows the measured second order rate constants versus NaCl concentration for two lengths of DNA (200 bp and 1000 bp). For both DNAs the rate is salt dependent, displaying a peak near 80 mM NaCl. The data show that the search rate depends on DNA length in a salt-dependent manner. Below 100 mM NaCl the rate increases with DNA length, with the longer DNA displaying faster target search. Above 100 mM NaCl the opposite trend is seen, with the longer DNA showing slower target search.

3.2. Verification of search rate measurements

We next verified that the variations in kinetics were due to target search and not to changes in the rate of DNA hydrolysis. To do this, we first identified a "peak" buffer in which the rate was a maximum. We reasoned that if we were to initiate a reaction under buffer conditions in which the reaction were slower, and then interrupted this halfway through to completion by washing out unbound enzyme with the peak buffer, then one of two results would follow. In the case of slow target search, the wash step would stop any further cleavage due to flushing out unbound enzyme. In the case of slow hydrolysis, the wash step would result in rapid cleavage of the remaining DNAs. We chose to use 80 mM NaCl and 2 mM $MgCl_2$ as our peak buffer (Fig. 2).

We tested the validity of this design by first performing the experiment in low magnesium, which is known to be essential for cleavage but not binding [24]. NdeI was injected into the flow channel in the presence of 80 mM NaCl/0.2 mM $MgCl_2$. As shown in Fig. 3A and S2A, the initial cleavage rate is low. However, upon injection of 80 mM NaCl/2 mM $MgCl_2$ rapid cleavage is induced, indicating that the initial slow kinetics are due to a reduction in the rate of hydrolysis and not binding to target. We then tested conditions that result in the slower kinetics shown in Fig. 2. We performed the experiment by injecting NdeI in buffer containing 2 mM $MgCl_2$ but either low (2 mM) or high (140 mM) NaCl (Fig. 3B–C and S2B–C). The initial cleavage in the presence of protein is similar to that in Fig. 3A. However, upon washing away protein with buffer containing 80 mM NaCl, cleavage rate reduces to the background bead loss rate indicating that the protein has not completely bound all DNA targets, consistent with slower search kinetics. Note that the slight increase in rate immediately after introducing the wash buffer (green line in Fig. 3) is due to the finite mixing time (~40s). During this time, residual enzyme remains in the flow cell as higher salt is mixed in creating a small drop in bead count.

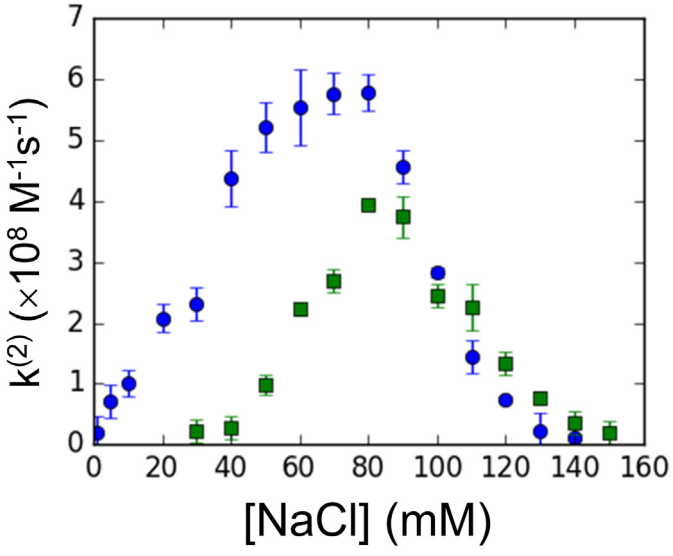

Fig. 2. Second order target search rates. Data for two lengths of DNA (200 bp: green squares, 1000 bp: blue circles) are shown. All data points represent means of at least three replicates. Only trials with at least 200 DNAs were included. Error bars represent standard errors in the mean. (For interpretation of the references to colour in this figure legend, the reader is referred to the Web version of this article.)

3.3. Salt concentration modulates the 1D sliding length of NdeI

To probe the effect of salt concentration on 1D search, we developed a method to block sliding using dCas9 (§S1), which binds target sites without cleaving DNA. The 1000 bp DNA was modified to include two identical roadblock sites, each containing a BtgI site, 100 bp upstream and downstream of the NdeI site (Fig. 1A and S1). We then targeted dCas9 to these sites using complementary sgRNAs. Control experiments with BtgI demonstrated 100% binding of dCas9 (Fig. S3A). In the absence of sliding, or if the sliding length is less than 100 bp, the presence of roadblocks will not affect the NdeI search rate. Fig. 4A & B shows the target search rate of NdeI in the presence and absence of roadblocks at low (40 mM) and high (100 mM) salt. The low salt condition shows significant slowing of target search in the presence of roadblocks, indicating sliding from farther than 100 bp is significant. At 100 mM salt, there is no difference due to the presence of roadblocks, demonstrating no significant sliding greater than 100 bp. This data confirms that salt varies the 1D sliding length of NdeI and that increasing salt decreases this length.

3.4. Modeling target search

We applied a two phase model to our data. In the 3D search phase the protein freely diffuses until it lands on a random location on the DNA. In the 1D search phase the protein searches a contiguous segment of the DNA via 1D diffusion until it either binds the target or dissociates to re-enter the 3D phase. The total search time is the number of search cycles multiplied by the average time per cycle. We assumed the protein can only reach its target via 1D search (direct landings on the site from the 3D phase are ignored). An iso-electric focusing gel (§S1.3) demonstrated that NdeI is negatively charged (pI = 5.6) in our buffers (pH = 7.6), suggesting electrostatic repulsion could play a role at low salt. We therefore included a salt dependent non-specific association rate assumed to increase by a power law [25,26]. An additional assumption was that the non-specific dissociation rate was determined by a power law dependence on salt concentration. This model leads to the following expression for the search time (§S2):

$$T = k^{-1} = \tau^{o}_{3D} \times \left\{ \left(\frac{[NaCl]}{[NaCl]_o} \right)^{-a} + N_o \times \left(\frac{[NaCl]}{[NaCl]_o} \right)^{q-a} \right\} \qquad (1)$$

In this equation, T is the search time, k is the first order DNA search rate, $[NaCl]_o$ is a reference salt concentration (100 mM), τ^{o}_{3D} is the time spent in a single cycle of 3D search at the reference salt concentration, $1 + N_o$ is equal to the number of search cycles at the reference salt concentration, and q and a are exponents that determine the salt dependence of the non-specific dissociation and association rates respectively.

A global fit of Eq. (1) demonstrates the ability of this model to explain our data (Fig. 4C). The model correctly describes the presence of a peak in the salt dependence. In addition, it correctly predicts the shift in peak (higher and to lower salt) as the DNA length is increased. Lastly, the model correctly accounts for the manner in which the search rate depends on DNA length at both

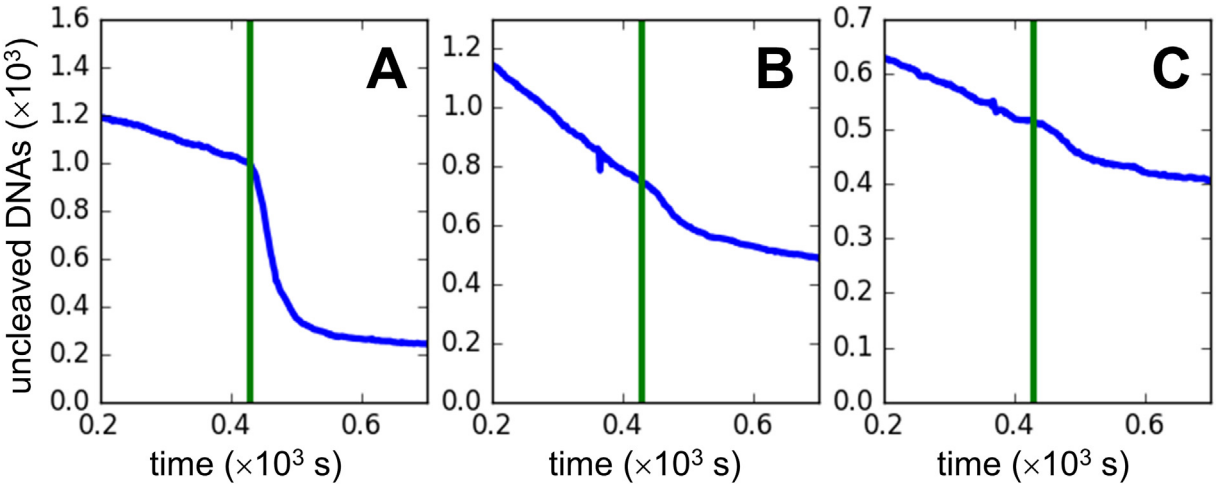

Fig. 3. Control experiments with 1000 bp DNA. Initial buffer and enzyme were washed out at ~420s (indicated by vertical green line) by wash buffer. (A) Initial buffer of 80 mM NaCl, 0.2 mM $MgCl_2$. (B) Initial buffer of 2 mM NaCl, 2 mM $MgCl_2$ and (C) initial buffer 140 mM NaCl, 2 mM $MgCl_2$. See Fig. S2 for data from 200 bp DNA. Variations in initial number of DNAs are due to normal statistical variations in tethering efficiency. (For interpretation of the references to colour in this figure legend, the reader is referred to the Web version of this article.)

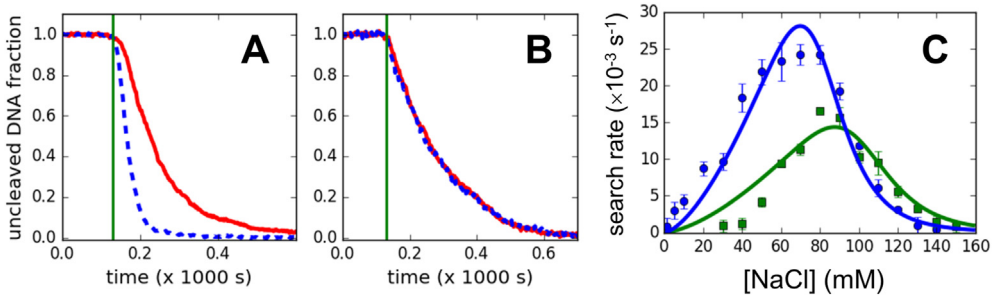

Fig. 4. (A) Target search kinetics in presence (solid) and absence (dashed) of roadblocks at 40 mM NaCl. Data is normalized (see Fig. S3 for raw data). (B) Same at 100 mM NaCl. (C) Model fit to data. The first order target search rates are plotted (200 bp DNA: green squares, 1000 bp DNA: blue circles) along with predictions of the model (green and blue solid curves) using the parameter values from Table 1. (For interpretation of the references to colour in this figure legend, the reader is referred to the Web version of this article.)

Table 1
Best fit values for model parameters as determined by numerical fits to data. See main text for description of parameters.

DNA length (bp)	τ^o_{3D} (s)	N_o	q	a
200	47.3 ± 3.8	0.67 ± 0.17	8.99 ± 0.86	1.53 ± 0.09
1000	17.1 ± 1.2	5.1 ± 1.2	8.99 ± 0.86	1.53 ± 0.09

low salt (where rate increases with DNA length) and high salt (where rate decreases with DNA length). The best fit parameters (Table 1) determine both the average time spent in each cycle of 3D search and the number of cycles needed to locate the target. As shown in the table, the 3D search time at the reference salt concentration (100 mM) for the 200 bp DNA (47.3 s) is roughly 2.8 times longer than that for the 1000 bp DNA (17.1 s). Similarly, at that salt concentration NdeI must undergo roughly 1.7 search cycles to effectively search the 200 bp, whereas it requires 6.1 cycles to search the longer 1000 bp DNA.

4. Discussion

One strategy for DNA target search employs a single cycle of 3D search followed by an effective and complete 1D search of the DNA. Assuming a rapid 1D phase, the search rate will equal the non-specific association rate. The rate will increase with increasing DNA length due to the "antenna" effect. At low salt (50 mM NaCl), EcoRI, BamHI and HindIII have all demonstrated increasing search rates as DNA length is increased, consistent with this strategy [15]. Below 80 mM NaCl, the target search rate of NdeI also increases with DNA length (Fig. 2), suggesting a similar strategy. Diffusion lengths as long as 1000 bp have been observed for both EcoRI [8] and LacI [6] in similar salt concentrations. In the case of NdeI, roadblocks 100 bp away from the target site slow search at 40 mM NaCl (Fig. 4A), indicating sliding from beyond that distance is significant. This can also explain why NdeI's search rate increases with salt concentration at low salt. Since NdeI is negatively charged under our assay conditions, ionic screening will reduce electrostatic repulsion as salt concentration increases, leading to faster target search.

In contrast to *in vitro* results, *in vivo* observations show DBPs make multiple short scans of DNA during target search. While LacI exhibits long scans *in vitro* [6,27], single molecule tracking in cells shows scans limited to 10s of bp either by dissociation or by roadblocks [5]. In the case of TetR, scans are 100s of bp in length [28]. In these cases, the search time is the time per search cycle multiplied by the number of cycles. Increased salt concentration will increase the number of cycles by reducing the fraction of the DNA scanned per encounter. This mechanism is supported by our data with roadblocks which show reduction in sliding length as salt

increases (Fig. 4A and B). In addition, above 80 mM NaCl the search rate falls dramatically with salt (Fig. 2). Increased DNA length will also increase the number of cycles required due to the increased number of non-specific sites which is also supported by our data above 100 mM (Fig. 2). One crucial component of this model, the reduction in 1D search efficiency with increasing salt, has been directly observed in EcoRI, where single molecule tracking has shown increasing salt leads both to a reduction in residence time and to an increase in hopping [8]. These effects combine to reduce the duration, length and efficiency of each individual 1D scan.

Our model shows quantitatively how salt concentration modulates search strategy. From Eq. (2), we find that the number of required cycles of 3D/1D search varies with salt concentration,

$$N = 1 + N_o \times \left(\frac{[NaCl]}{[NaCl]_o}\right)^q \quad (2)$$

In this equation, N is the total number of search cycles, and N_o and q are defined as before. The critical salt concentration where NdeI switches behavior is determined by when the number of additional cycles *N-1* first becomes significant as salt is increased. Setting this equal to 0.1, we find a critical salt concentration of 83 mM for the 200 bp DNA, and 69 mM for the 1000 bp DNA (parameters from Table 1). These salt concentrations coincide with the peaks in the search rate which mark the transition between the two behaviors. Below the critical salt concentration, the DBP makes a single efficient scan of the DNA after its initial landing. At higher salt concentration, multiple scans must be made. For example, at 150 mM NdeI must perform ~20 search cycles for the 200 bp DNA, whereas for the 1000 bp DNA it must make ~70. In the simplest picture, one might expect the ratio of search cycles for the two DNAs at high salt to be equal to the ratio of their lengths, 5, whereas the actual number is closer to 3.5. The difference could be due to the contribution of jumping which has been shown to increase the search rate of EcoRV [19]. Longer DNAs will exhibit more coiling which will provide more opportunity for rebinding of the protein once it dissociates but before it wanders away from the DNA coil.

While prior work has shown how salt concentration can affect the 1D search, our results demonstrate how this mechanism modulates the overall search strategy including both 3D and 1D search. The model resolves the conflict between *in vitro* data at low salt (<75 mM) which suggests proteins make highly efficient scans of DNA with *in vivo* results at cellular salt conditions (130–270 mM [29]) that show DBPs make multiple scans during target search. The two strategies predict very different dependencies on DNA length and salt concentration and can be understood as two limits of the same underlying behavior. Interesting questions remain as to why particular strategies are chosen *in vivo* where DNA conformation and roadblocks may have important roles.

Declaration of competing interest

The authors declare that they have no known competing financial interests or personal relationships that could have appeared to influence the work reported in this paper.

Acknowledgments

The authors thank John F. Marko for fruitful discussion concerning the interpretation of our data. This work was supported by the National Science Foundation grant MCB-1715317.

Appendix A. Supplementary data

Supplementary data to this article can be found online at https://doi.org/10.1016/j.bbrc.2020.10.036.

References

[1] O.G. Berg, R.B. Winter, P.H. Von Hippel, Diffusion-driven mechanisms of protein translocation on nucleic acids. 1. Models and theory, Biochemistry 20 (1981) 6929–6948.
[2] S.E. Halford, J.F. Marko, How do site-specific DNA-binding proteins find their targets? Nucleic Acids Res. 32 (2004) 3040–3052.
[3] K.V. Klenin, H. Merlitz, J. Langowski, C.-X. Wu, Facilitated diffusion of DNA-binding proteins, Phys. Rev. Lett. 96 (2006), 018104.
[4] R.B. Winter, O.G. Berg, P.H. Von Hippel, Diffusion-driven mechanisms of protein translocation on nucleic acids. 3. The Escherichia coli lac repressor-operator interaction: kinetic measurements and conclusions, Biochemistry 20 (1981) 6961–6977.
[5] P. Hammar, P. Leroy, A. Mahmutovic, E.G. Marklund, O.G. Berg, J. Elf, The lac repressor displays facilitated diffusion in living cells, Science 336 (2012) 1595–1598.
[6] Y. Wang, R.H. Austin, E.C. Cox, Single molecule measurements of repressor protein 1D diffusion on DNA, Phys. Rev. Lett. 97 (2006), 048302.
[7] D.C. Rau, N.Y. Sidorova, Diffusion of the restriction nuclease EcoRI along DNA, J. Mol. Biol. 395 (2010) 408–416.
[8] S.C. Piatt, J.J. Loparo, A.C. Price, The role of noncognate sites in the 1D search mechanism of EcoRI, Biophys. J. 116 (2019) 2367–2377.
[9] B. Terry, W. Jack, P. Modrich, Facilitated diffusion during catalysis by EcoRI endonuclease. Nonspecific interactions in EcoRI catalysis, J. Biol. Chem. 260 (1985) 13130–13137.
[10] L.J. Friedman, J.P. Mumm, J. Gelles, RNA polymerase approaches its promoter without long-range sliding along DNA, Proc. Natl. Acad. Sci. Unit. States Am. 110 (2013) 9740–9745.
[11] H. Ghodke, H. Wang, C.L. Hsieh, S. Woldemeskel, S.C. Watkins, V. Rapić-Otrin, B. Van Houten, Single-molecule analysis reveals human UV-damaged DNA-binding protein (UV-DDB) dimerizes on DNA via multiple kinetic intermediates, Proc. Natl. Acad. Sci. Unit. States Am. 111 (2014) E1862–E1871, https://doi.org/10.1073/pnas.1323856111.
[12] M.R. Tock, D.T. Dryden, The biology of restriction and anti-restriction, Curr. Opin. Microbiol. 8 (2005) 466–472.
[13] A. Pingoud, M. Fuxreiter, V. Pingoud, W. Wende, Type II restriction endonucleases: structure and mechanism, Cell. Mol. Life Sci. 62 (2005) 685–707.
[14] W.E. Jack, B.J. Terry, P. Modrich, Involvement of outside DNA sequences in the major kinetic path by which EcoRI endonuclease locates and leaves its recognition sequence, Proc. Natl. Acad. Sci. Unit. States Am. 79 (1982) 4010–4014.
[15] H.-J. Ehbrecht, A. Pingoud, C. Urbanke, G. Maass, C. Gualerzi, Linear diffusion of restriction endonucleases on DNA, J. Biol. Chem. 260 (1985) 6160–6166.
[16] N.P. Stanford, M.D. Szczelkun, J.F. Marko, S.E. Halford, One-and three-dimensional pathways for proteins to reach specific DNA sites, EMBO J. 19 (2000) 6546–6557.
[17] D.M. Gowers, S.E. Halford, Protein motion from non-specific to specific DNA by three-dimensional routes aided by supercoiling, EMBO J. 22 (2003) 1410–1418.
[18] D.M. Gowers, G.G. Wilson, S.E. Halford, Measurement of the contributions of 1D and 3D pathways to the translocation of a protein along DNA, Proc. Natl. Acad. Sci. U. S. A. 102 (2005) 15883–15888.
[19] B. van den Broek, M.A. Lomholt, S.-M. Kalisch, R. Metzler, G.J. Wuite, How DNA coiling enhances target localization by proteins, Proc. Natl. Acad. Sci. Unit. States Am. 105 (2008) 15738–15742.
[20] A.M. van Oijen, Single-molecule approaches to characterizing kinetics of biomolecular interactions, Curr. Opin. Biotechnol. 22 (2011) 75–80.
[21] G.J. Gemmen, R. Millin, D.E. Smith, Tension-dependent DNA cleavage by restriction endonucleases: two-site enzymes are “switched off” at low force, Proc. Natl. Acad. Sci. Unit. States Am. 103 (2006) 11555–11560.
[22] S. Gambino, B. Mousley, L. Cathcart, J. Winship, J.J. Loparo, A.C. Price, A single molecule assay for measuring site-specific DNA cleavage, Anal. Biochem. 495 (2016) 3–5.
[23] E.K. Matozel, N. Dale, A.C. Price, Parallel high throughput single molecule kinetic assay for site-specific DNA cleavage, JoVE: JoVE (2020).
[24] A. Pingoud, A. Jeltsch, Recognition and cleavage of DNA by type-II restriction endonucleases, Eur. J. Biochem. 246 (1997) 1–22.
[25] O.G. Berg, C. Blomberg, Association kinetics with coupled diffusion: III. Ionic-strength dependence of the lac repressor-operator association, Biophys. Chem. 8 (1978) 271–280.
[26] T.M. Lohman, P.H. von Hippel, Kinetics of protein-nucleic acid interactions: use of salt effects to probe mechanisms of interactio, CRC Crit. Rev. Biochem. 19 (1986) 191–245.
[27] A. Tempestini, C. Monico, L. Gardini, F. Vanzi, F.S. Pavone, M. Capitanio, Sliding of a single lac repressor protein along DNA is tuned by DNA sequence and molecular switching, Nucleic Acids Res. 46 (2018) 5001–5011.
[28] D. Normanno, L. Boudarene, C. Dugast-Darzacq, J. Chen, C. Richter, F. Proux, O. Bénichou, R. Voituriez, X. Darzacq, M. Dahan, Probing the target search of DNA-binding proteins in mammalian cells using TetR as model searcher, Nat. Commun. 6 (2015) 7357.
[29] D. Szatmári, P. Sárkány, B. Kocsis, T. Nagy, A. Miseta, S. Barkó, B. Longauer, R.C. Robinson, M. Nyitrai, Intracellular ion concentrations and cation-dependent remodelling of bacterial MreB assemblies, Sci. Rep. 10 (2020) 1–13.